atmosphere

MDPI

*Review*

# Space Weather Effects on the Earth's Upper Atmosphere: Short Report on Ionospheric Storm Effects at Middle Latitudes

**Ioanna Tsagouri**

National Observatory of Athens, Institute for Astronomy, Astrophysics, Space Applications and Remote Sensing, Metaxa & Vas. Pavlou, 15236 Penteli, Greece; tsagouri@noa.gr

**Abstract:** During geomagnetic storm events, the highly variable solar wind energy input in the magnetosphere significantly alters the structure of the Earth's upper atmosphere through the interaction of the ionospheric plasma with atmospheric neutrals. A key element of the ionospheric storm-time response is considered to be the large-scale increases and decreases in the peak electron density that are observed globally to formulate the so-called positive and negative ionospheric storms, respectively. Mainly due to their significant impact on the reliable performance of technological systems, ionospheric storms have been extensively studied in recent decades, and cumulated knowledge and experience have been assigned to their understanding. Nevertheless, ionospheric storms constitute an important link in the complex chain of solar-terrestrial relations. In this respect, any new challenge introduced in the field by a better understanding of the geospace environment, new modeling and monitoring capabilities and/or new technologies and requirements also introduces new challenges for the interpretation of ionospheric storms. This paper attempts a brief survey of present knowledge on the fundamental aspects of large-scale ionospheric storm time response at middle latitudes. Further attention is paid to the results obtained regarding the critical role that solar wind conditions which trigger disturbances may play on the morphology and the occurrence of ionospheric storm effects.

**Keywords:** space weather; ionosphere; ionospheric storms



**Citation:** Tsagouri, I. Space Weather Effects on the Earth's Upper Atmosphere: Short Report on Ionospheric Storm Effects at Middle Latitudes. *Atmosphere* **2022**, *13*, 346. https://doi.org/10.3390/atmos13020346

Academic Editors: Panagiota Preka-Papadema and Chris G. Tzanis

Received: 31 December 2021
Accepted: 14 February 2022
Published: 18 February 2022



## 1. Introduction

The Earth's ionosphere is the ionized part of the upper atmosphere, extending from about 60 km to 1000 km altitude imbedded in the neutral atmosphere. Ionospheric ionization is produced and further stratified through solar radiation, with the maximum concentration of the ionization to occur in the ionospheric F region. As the inner edge of the magnetosphere with clear links to the neutral atmosphere, the ionosphere plays a critical role in solar-terrestrial relationships, merging the influence from both above and below. In this respect, the transient changes imposed by space weather events in the near-Earth space environment lie among most challenging topics for both scientific and operational applications, e.g., [1–3].

During disturbed space weather conditions, the highly variable solar wind energy input in the magnetosphere significantly impacts the upper atmosphere's state through the interaction of the ionospheric plasma with atmospheric neutrals. Most dramatic changes follow the occurrence of geomagnetic storms, during which, a variety of photo-chemical and chemical reactions, as well as dynamical and electrodynamical processes that are activated in the magnetosphere-ionosphere-thermosphere system, drive the exchange and transportation of mass, momentum, and energy between the system's elements, and consequently, substantially alter the ionospheric structure. A key element of the ionospheric response to geomagnetic storm events comes in the form of disturbances in the peak electron density (NmF2) and column density (i.e., the total electron content—TEC): large-scale increases and decreases in the two parameters are observed globally to formulate the so-called positive and negative ionospheric storms, respectively.

Both the origin and the occurrence of the ionospheric storms have been subject to many studies during recent decades. The community's interest is justified by the significant impact of ionospheric storm effects on the reliable performance of technological systems, while it is further fed by the scientific challenges that are met in their investigation along the complex chain of solar-terrestrial relations. Negative ionospheric storm effects (i.e., NmF2 and TEC decrease well below their normal levels) cause serious problems in ground-based HF radio communications, while on the other hand, positive ionospheric storm effects (i.e., NmF2 and TEC increase well above their normal levels) can cause serious problems such as time delay, range error, and scintillations in satellite communication and navigation [4]. On the other hand, a set of dependencies (e.g., seasonal, local time, latitudinal, altitudinal) compile a rather complicated scene for the appearance of ionospheric storm effects to keep the relevant topic a vivid research field.

This paper attempts a brief survey of present knowledge on key aspects of ionospheric storms with the emphasis in the ionospheric storm effects at middle latitudes and the F region. Recent results and some additional evidence dealing with the critical role of the solar wind conditions that trigger the geomagnetic and ionospheric storm activity are also discussed. The paper is structured as follows: materials and methods used in the analysis are presented in Section 2, while the results are provided in Section 3, and are further discussed in Section 4, together with some suggestive concluding remarks.

## 2. Materials and Methods

This work is greatly based on bibliographic research. Complementary results are obtained through the analysis of two ionospheric characteristics; the peak electron density in terms of the critical frequency foF2, and the height of the peak electron density hmF2 obtained by a network of European stations listed in Table 1. foF2 is related to the F-peak electron density NmF2 by $NmF2/m^{-3} = 1.24 \times 10^{10} \times (foF2/MHz)^2$. The analyzed period includes the years 2008–2020 that fully cover the evolution of solar cycle 24 (see also Figure 1). Ionospheric disturbances are justified through the comparison between the observed values with their monthly medians. Disturbances are quantified by the following metric: DfoF2% = [(foF2obs − foF2median)/foF2median] × 100 for foF2.

**Table 1.** List of the ionospheric stations used in the analysis and their geographic coordinates.

| Station Name | Geographic Longitude (°E) | Geographic Latitude (°N) |
|---|---|---|
| Chilton | 359.4 | 51.5 |
| Dourbes | 4.6 | 50.1 |
| Juliusruh | 13.4 | 54.6 |
| Pruhonice | 14.6 | 50.0 |
| Ebre | 0.5 | 40.8 |
| Rome | 12.5 | 41.9 |
| San Vito | 17.8 | 40.6 |
| Athens | 23.5 | 38.0 |

Ionospheric observations were retrieved from the Global Ionosphere Radio Observatory (GIRO—http://giro.uml.edu/, accessed on 30 December 2021) data repository [5], particularly the FastChart database. The level of the geomagnetic activity is determined by records of Dst index available from the World Data Center (WDC) for Geomagnetism, Kyoto (http://wdc.kugi.kyoto-u.ac.jp/dstdir/, accessed on 30 December 2021). Geomagnetic storms may be grouped with respect to their intensity, as in Table 2.

**Table 2.** Classification of storm events.

| Dst min (nT), Range | Storm Intensity |
|---|---|
| −30 to −50 | Weak |
| −50 to −100 | Moderate |
| <−100 | Intense |

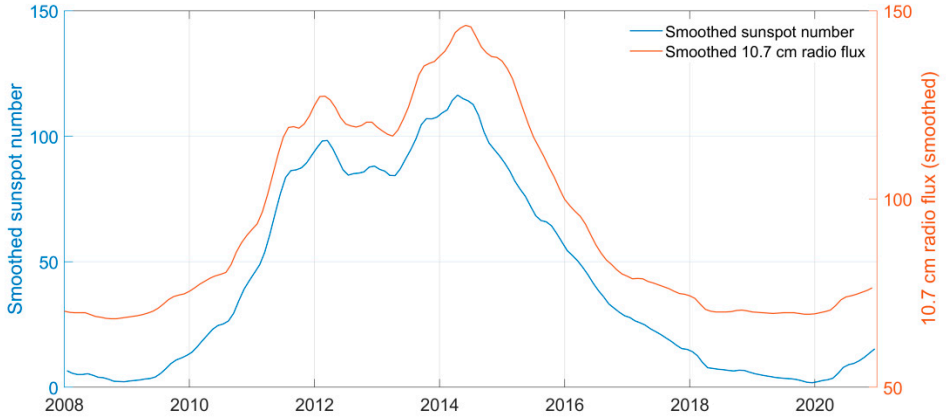


**Figure 1.** The smoothed monthly solar sunspot number provided by the World Data Center(WDC) Sunspot Index and Long-Term Solar Observations (SILSO) in Royal Observatory of Belgium and the smoothed 10.7 cm radio flux provided by SWPC (Space Weather Prediction Center) in NOAA (National Oceanic and Atmospheric Administration) for the time interval 2008–2020. Solar cycle 24 started in December 2008, following a deep and long solar minimum. It reached its maximum in April 2014 and ended in December 2019.

## 3. Results

Geomagnetic storms are initiated by the arrival of geo-effective solar wind flows at the Earth's vicinity (see, for instance [6–15]). Geo-effectiveness is determined by a combination of solar wind velocity and southward orientation of the Interplanetary Magnetic Field (IMF), with the second to hold the most important role because of its far greater variability. Magnetic reconnection is the key physical process responsible for transferring solar wind energy into the magnetosphere during geomagnetic storms, being strongest under southward IMF orientation: southward directed IMF interconnects with the Earth's magnetopause northward magnetic field and solar wind drags the interconnected magnetic fields and plasma downstream (i.e., in the antisunward direction); the open magnetic fields then reconnect in the magnetotail. The relative rate of the reconnection in the magnetopause and magnetotail sets off a global convection cycle of magnetic flux between the dayside and nightside magnetosphere. The convection cycle (also known as Dungey cycle [16]) and related disturbances induce plasma instabilities, wave growth and wave-particle interactions, also giving rise to a wide range of global processes, including the build-up of storm-time ring current, the activation of the field-aligned current system and the auroral electrojects, the variability of radiation belt intensities, and enhanced particle precipitation into lower latitudes. Through such processes, the magnetospheric disturbances are projected down to the ionosphere. The stronger the southward IMF component and the stronger the solar wind velocity convecting the magnetic field, the more strongly the solar-wind-magnetosphere-ionosphere system is driven. This dependence is reflected in the magnetospheric energy input functions, such as the epsilon parameter of Akasofu, the most widely used one, according to which the solar wind energy input is determined by the solar wind speed, the IMF magnitude, and the so-called clock angle of the IMF orientation perpendicular to the Sun-Earth line [17–19]. The solar wind energy entering the magnetosphere is then dissipated via a variety of dynamic processes in the plasma sheet, the ring current and the ionosphere, with the latter being the dominant sink of the solar wind

energy input through storm currents and particle precipitation, both contributing to the heating of the upper atmosphere. This energy dissipation in the high-latitude ionosphere generates numerous upper atmospheric changes that affect all state parameters.

Key mechanisms which are the main sources of geo-effective solar wind flows include [6–15]: (i) coronal mass ejections (CMEs) and the interplanetary CMEs (ICMEs), the evolutionary part of CMEs as they propagate through interplanetary space, as well as fast sheaths and shocks upstream of CMEs/ICMEs. Such structures occur more often near the solar maximum, carrying embedded southward-directed IMF at the Earth's vicinity. (ii) High-speed (~750–800 km/s) solar wind streams (HSSs) emanating from solar coronal holes and corotating interaction regions (CIRs). CIRs are associated with HSSs that interact with slow-speed (~300–400 km/s) streams and are characterized by embedded and amplified Alfvén waves. CIRs usually lead to weak or moderate geomagnetic storms, mainly in the declining phase of the solar cycle. Moreover, they tend to evolve gradually and recover in longer time scales than CME-driven events. It is suggested that the CIR storms are driven by the magnetic reconnection of the southward component of the interplanetary Alfvén waves to the Earth's dayside magnetopause fields [6–15].

### *3.1. Ionospheric Storms—Morphology and Background Mechanisms*

The main drivers of the ionospheric disturbances during a geomagnetic storm can be roughly categorized by four different methods: (i) enhanced high-energy particle precipitation; (ii) enhanced ionospheric electric currents and resulting Joule heating; (iii) enhanced electric fields; (iv) frictional heating at high latitudes, primarily induced by enhanced magnetospheric convection. While the direct effects of these mechanisms are mainly important at high and maybe at low (see for instance electric fields) latitudes, it has been argued that Joule and particle heating is globally the most critical factor causing the F region effects of geomagnetic storms [20–23]. Such effects are still activated in high latitudes, but they are transported to lower latitudes through wind circulation and waves [21].

Long-lasting negative storm effects are the most typical feature of the ionospheric storm time response. Driven by the initial dependence of the ground-based communications on HF radio, the negative storms were the first to receive the community's attention. Today, it is believed that the physical mechanisms of the negative storms are more or less understood, and negative ionospheric storm effects are mainly attributed to changes in neutral gas composition. In this scenario, the Joule and particle heating in the high-latitude region causes thermal expansion. In this way, large temperature and pressure gradients drive horizontal winds that produce global changes in the thermospheric circulation, with the storm-induced winds blowing from high to low latitudes. The divergence of the winds at subauroral latitudes causes the upwelling of neutral gas in the thermosphere, and by transporting neutral molecules into much higher altitudes, produces a neutral composition disturbance zone (also known as "composition bulge") and decreases the ionospheric ionization at F region heights [21,24–26].

Neutral composition changes are present even during geomagnetically quiet conditions, but confined in the polar region. They are relatively small and restricted to subauroral latitudes, even during moderately disturbed geomagnetic conditions, especially in the daytime sector. Both the amplitude and the extent of the composition changes increase with increasing geomagnetic activity, and they are transported to lower latitudes by both the storm-induced and regular wind circulation [21,24].

Contrary to the case of negative ionospheric storms, positive storms have proven to be more challenging in their explanation. Even today, the research community has not arrived at a generally accepted explanation for their origin. Possible mechanisms proposed in the literature for the explanation of the observed positive storm effects mainly include [21–23,25,27,28]:

i. Neutral composition changes through the downwelling of neutral gas due to the convergence of neutral winds;
ii. F layer uplifting due to vertical drifts. An increase in layer height leads to an increase in ionization density due to the reduced rate of ionization loss at higher altitudes. The F layer drift may be caused by two principal mechanisms:
    - Equatorward-directed winds: in this case, the ions and electrons feel a frictional force. The geomagnetic field-aligned component of this force pushes the ionization up to the inclined magnetic field lines, resulting in an uplifting of the F layer. Such winds may be caused either by large-scale wind circulation or as part of so-called traveling atmospheric disturbances (TADs). TADs are the superimposed result of impulse-like travelling disturbances formed by a wide spectrum of atmospheric gravity waves. These are launched by the injection of solar wind energy to the polar upper atmosphere. TADs propagate with high velocity towards lower latitudes carrying along equatorward-directed winds of moderate magnitude.
    - Electric fields: in this case, the height increase is caused by an ExB drift that is perpendicular to the inclined geomagnetic field, so it also leads to an uplifting of the ionosphere. Two major disturbance electric fields are: a. Disturbance dynamo electric fields: the disturbed thermospheric winds drive meridional winds to generate electric fields opposed to their quiet-time patterns. b. Penetration of electric fields originated from the solar wind/magnetosphere: high-latitude convection electric fields penetrate into the low-latitude ionosphere (a phenomenon known as prompt penetration electric fields, PPEFs) to produce changes known as the super-fountain effect [29].
iii. Advection of high-density plasma in combination to plasma uplift: nightside plasma is carried across the sunset terminator to draw out plumes of storm-enhanced density (SED) that stretches from the dusk sector to the noontime cusp ionosphere [30].
iv. Downward plasma flux from the plasmasphere.

Most probably, all these mechanisms may be considered important, with relevant contributions to the occurrence of positive ionospheric storms. However, vertical plasma drifts can also explain the observed increase in layer height that usually accompanies positive effects, and in this respect, they are claimed to be the dominant ones [21]. Among them, it has been suggested that thermodynamics may be more important for disturbances at the peak electron density height, while electrodynamics may more efficiently control the disturbances above [23] with the penetration fields, to play a significant role in the development of positive storms during the initial phase of the storm, in the afternoon sector, and at middle-to-low and low latitudes [22]. In any case, the relative importance of equatorward winds and electric fields in the generation of ionization increases, especially in the middle latitudes, remains among present challenges, and is not yet fully understood.

### *3.2. On the Occurrence of the Ionospheric Storm Effects*

The occurrence of ionospheric storm effects is subject to several dependences for which the regular thermospheric winds play a key role. As an example, one may note the seasonal dependence: when storm-induced wind flow coincides with the direction of the prevailing meridional wind, which is the case for summer, the neutral composition disturbance zone penetrates to relatively low latitudes, and negative storms can also be observed at lower latitudes. On the other hand, in winter, the prevailing wind contrasts with storm-induced wind and, therefore, negative storm effects remain confined at higher latitudes to make positive effects the predominant feature of wintertime ionospheric storms [24–26,28].

Another key feature in the ionospheric storms occurrence is their dependence on local time. Neutral composition changes tend to be larger and extend to lower latitudes in the early morning sector. This is in agreement with the argument that the disturbance transport takes place in this sector due to the reduced ion drag and coincidence of the equatorward regular wind with storm-induced wind flow. In this respect, negative storm effects at middle latitudes are mainly observed during nighttime hours. While rotating into the daytime sector following the Earth's rotation, the disturbance zone is partially recovered and pushed back by poleward-directed daytime regular winds, but it is still able to produce daytime negative ionospheric storm effects. On the other hand, positive storm effects tend to occur in the daytime hemisphere, particularly in the prenoon and afternoon sectors [24,25,28].

Figure 2 provides an example of how positive and negative storm phases may alternate in different local time sectors and/or latitudes. For a more representative view of the ionospheric response to this intense storm event, the reader can refer to several research articles available in the literature, e.g., [31–33]. Multi-instrument data analysis and physics-based model simulations are also carried out for other intense storm events that occurred in solar cycle 24, e.g., [34–36] provide the most recent evidence on the progress achieved in our present understanding, but also on the complexity that one may face in practice. Indeed, the sequence of ionospheric storm effects may be very complicated as several different processes work in concert, and the ionospheric response to each storm is determined by a unique and complex interaction of drivers, while multiple and/or successive intensifications of the geomagnetic activity may further complicate the interpretation of the observed effects, e.g., [37].

It has also been suggested that ionospheric storm effects are subject to solar cycle dependence. At the beginning of the 2000s, this argument was only based on model predictions. For instance, Burns et al. [38] found that, considering winter conditions, both the magnitude and extent of composition perturbations were larger during solar minimum, suggesting that disturbance effects are transported more efficiently out of the polar region into middle latitudes during these conditions. Interest in the solar cycle dependence of the ionospheric storm time response was greatly revived in the years following the deep 2008–2009 solar minimum, and probably the low activity solar cycle 24. Some indicative results came from identified shortcomings in ionospheric prediction capabilities during this deep solar minimum, under certain conditions that apply to all model formulations, from empirical to physics-based ones. For instance, Buresova et al. [39], in an investigation of the ionospheric disturbances under low solar activity conditions in 2008–2009, pointed out that the STORM model [40,41]—incorporated into the International Reference Ionosphere (IRI) standard model—did not provide reliable predictions for the peak electron density during CIR-generated storms. Wang et al. [42] also reported that the Coupled Magnetosphere Ionosphere Thermosphere (CMIT) model was not sufficiently able to reproduce the F2 peak electron density variations observed during the CIR events that occurred during the Whole Heliosphere Interval in 2008 (Day of Year 50–140). Such results may be considered to be suggestive of different ionospheric response to different levels of solar activity and/or different ionospheric response to geomagnetic storms driven by different solar/interplanetary conditions. The latter was also supported by the results obtained through the assessment of the Solar Wind-driven Autoregression Model for Ionospheric Forecast (SWIF) [43–45]. In particular, it was found that, while ionospheric disturbances related to the occurrence of CME-driven storms in the ascending phases of the solar cycles 23 and 24 were successfully predicted by the SWIF model, the performance of the model was significantly poorer during non-CME related ones which occurred in the same solar activity phase [46].

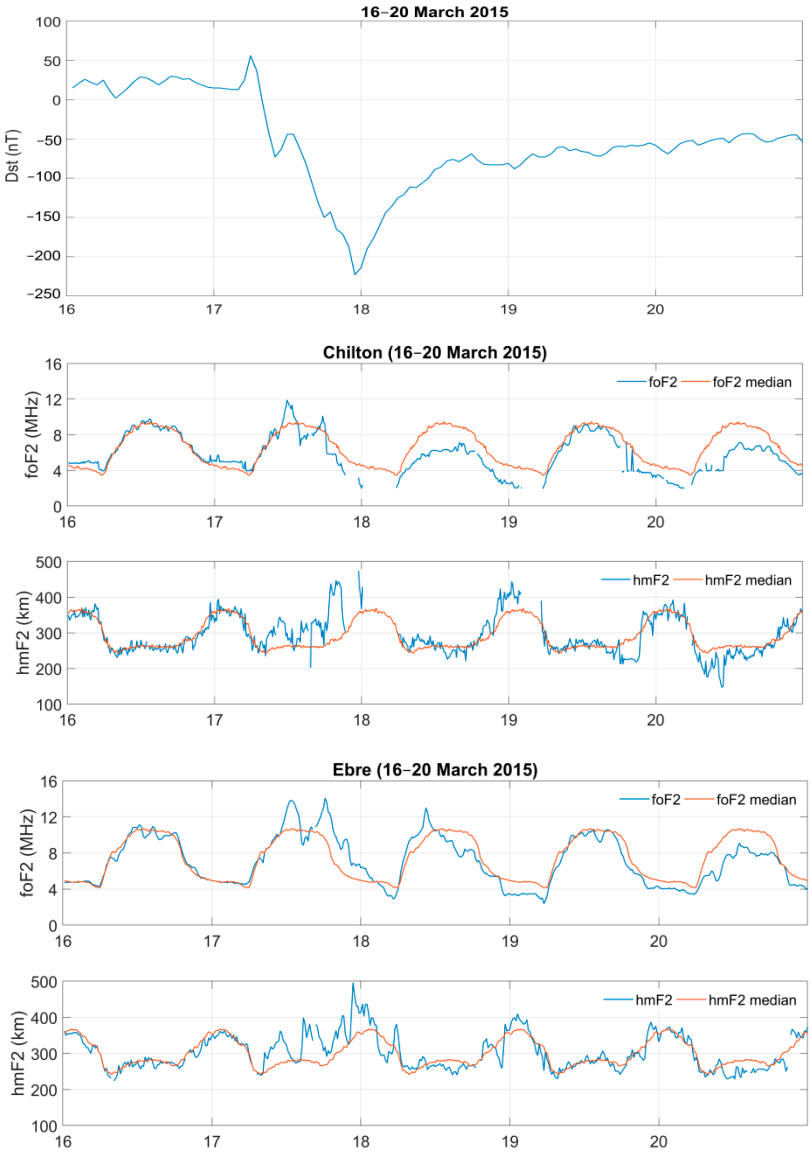


**Figure 2.** The ionospheric response over Europe to the intense geomagnetic storm (min Dst -223 nT) that occurred in the time interval 16–20 March 2015. This was the greatest geomagnetic storm of solar cycle 24. Top panel: The variation of the Dst index. Middle panel(s): the variation of foF2 and hmF2 ionospheric characteristics in comparison to their monthly medians over Chilton. Bottom panel(s): the variation of foF2 and hmF2 ionospheric characteristics in comparison to their monthly medians over Ebre. The two stations are located in the same local time sector. The F2 layer is uplifted at both ionospheric locations during the storm main phase. Impulse-like increases in the height of the peak electron density are related to similar increases in the ionospheric ionization (positive storm effects) on 17 March. The effects are more intense at lower latitudes (i.e., over Ebre). One may also note two qualitative differences in the response over the two distinct locations: (i) the positive storm penetrates the evening sector at lower latitudes, while at Chilton, it remains confined to daytime hours; (ii) Chilton experiences strong negative storm effects (foF2 is reduced by up to 50% with respect to the normal values) on the second storm day, most probably by entering the disturbance zone in the evening hours, while Ebre recovers to normal conditions.

The work performed by Tsagouri et al. [47] supported an investigation of the long-term behavior of the ionospheric disturbances during the ascending phase of solar cycle 24 (i.e., for the time interval 2008–2014) with two objectives: the analysis of the ionospheric behavior in a wide range of geophysical conditions, and the determination of specific features that

may differentiate the ionospheric response to different faces of space weather driving. By extending a key part of their analysis here, Figure 3 provides the annual distribution of the DfoF2 as a metric of the ionospheric activity for the years 2008–2020. The results verify that significant ionospheric disturbances (greater than 20% with respect to normal conditions) are recorded during all years, even in extremely low solar activity conditions mainly capturing the impact of geo-effective solar wind structures. Furthermore, the results indicate that there are qualitative differences in the ionospheric activity between different levels of solar activity: the intensity of the positive disturbances tends to be higher during the years of low solar activity and solar minima (i.e., 2008–2010 and 2017–2019) compared to the solar maximum years (2012–2014), while they clearly dominate numerically over the negative disturbances. More generally, it was suggested that during low solar activity and solar minimum, the solar wind impact on the geospace environment particularly favors the occurrence of ionization increases, both in frequency and intensity. Ionization depletions are still present, but they mainly appear in moderate intensity, in contrast with the situation in solar maximum. The ionization increases were apparent in all local time sectors, while they clearly dominated in the afternoon hours, and they were accompanied only partially by an increase in the F2 layer peak electron density height (hmF2) [47]. Although it is known that the afternoon ionization enhancements observed during storm conditions, when portrayed as a percentage change, are inversely related to solar flux, simply because of the monthly median control curves having smaller magnitudes (i.e., net solar cycle effect) [22], the identified differences were better attributed to different solar wind drivers: positive disturbances with strong afternoon components tend to be a critical feature of the ionospheric response to the impact of CIR/HSSs in the ionospheric middle latitudes that tend to dominate during the declining solar cycle phase and solar minimum conditions.

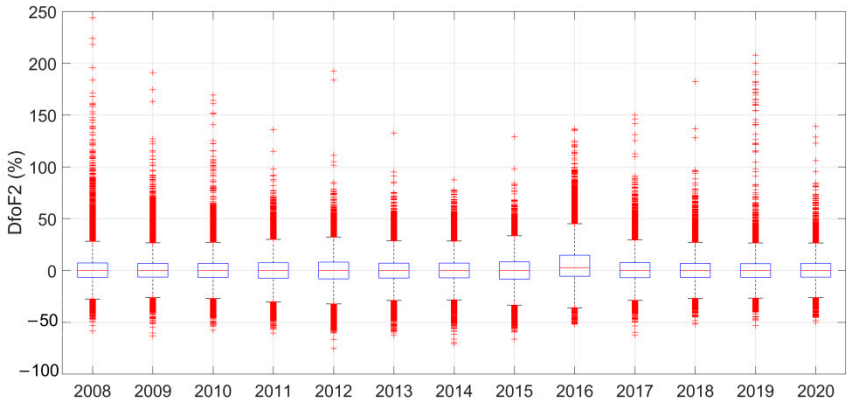


**Figure 3.** The annual distributions of the DfoF2 estimates obtained over European locations for each year of the considered time period (i.e., 2008–2020) in a box plot format. The box has lines at the lower quartile, median (red line), and upper quartile values. Whiskers extend from each end of the box to the adjacent values in the data; in our case, to the most extreme values within 1.5 times of the interquartile range from the ends of the box. Outliers (e.g., data with values beyond the ends of the whiskers) are presented by red crosses.

Similar results have also been reported at several occasions for middle latitudes. As indicative cases, we note: Buresova et al. [39] reported mainly positive disturbances in terms of the peak electron density under the occurrence of CIR-generated storms that occurred in the low solar activity years 2008–2009, with no significant changes in hmF2 in several cases; Burns et al. [48] found positive effects of geomagnetic storms in the peak electron density of the ionospheric F2 layer in the main storm days during CIR/HSSs-driven events; Dimitriev et al. [49] and Verkhoglyadova et al. [50,51] revealed the close relationship between the positive ionospheric storms and recurrent geomagnetic activity; Matamba and Habarulema [52] concluded that positive ionospheric storm effects in terms of GPS-derived TEC were more prevalent over middle, low and equatorial latitude stations during

both CME- and CIR-driven storms, while negative ionospheric storm effects occurred only during CME-driven storms at the considered Southern and Northern Hemisphere middle latitudes.

## 4. Discussion and Conclusive Remarks

This paper attempts to provide a brief survey of knowledge on ionospheric storms, with the emphasis on the ionospheric effects at middle latitudes and the F region. As the ionosphere merges the influence from both above (solar wind/magnetosphere) and below (neutral atmosphere), ionospheric storms act as an important link in the complex chain of solar-terrestrial relations. In this respect, their investigation establishes a wide field of research that combines interdisciplinary expertise and/or knowledge. To keep the present survey brief, but at the same time, as complete as possible, the discussion is developed in a rather simplified way. For a fully justified overview of the present understanding on the ionospheric storms morphology and background mechanisms, the reader is urged to refer to extended reviews, collections of papers or chapter books available in the literature [1,21–25,27,53,54].

Following many years of investigation, the physical mechanisms for the origin and occurrence of ionospheric storm effects are more or less in place. The situation is clearer in case of negative ionospheric storm effects, which are mainly attributed to changes in the neutral gas composition that are driven by Joule, and particle heating in the high-latitude region and consequent thermal expansion. Positive storm effects are more complicated in their explanation. They can be activated either also by neutral composition changes or the F layer uplifting, due to vertical drifts that bring the F layer higher where the rate of ionization loss is lower. The F layer drift may be caused by two principal mechanisms: equatorward-directed winds and electric fields (disturbance dynamo electric fields or the penetration of electric fields originated from the solar wind/magnetosphere). The advection of high-density plasma can take place in combination with plasma uplift, or through the interaction with the plasmasphere, and further explain observed ionization increases. Among the proposed mechanisms, vertical drifts seem to be the dominant ones, but the relative importance of equatorward winds and electric fields in the generation of ionization increases, especially in the middle latitudes, is still an open issue for the research community.

The occurrence of ionospheric storm effects is subject to several dependencies. Today, seasonal and local time dependencies are rather well justified and satisfactorily interpreted through the relative blow of storm-induced and regular thermospheric winds that keep the neutral composition disturbances confined to higher latitudes during daytime hours and the winter season. One of the key challenges in the investigation of the ionospheric storms in the last decade has been their solar cycle dependence. At the beginning of the 2000s, this dependence was rather an assumption based on model predictions [21,38]. However, interest in the solar cycle effect on the ionospheric storm time response was greatly revived in the years following the deep 2008–2009 solar minimum, and probably the low activity solar cycle 24. Shortcomings in ionospheric prediction capabilities during this deep solar minimum that were identified for all types of model formulations (from empirical to physics-based ones), the investigation of the long-term behavior of the ionospheric disturbances in solar cycle 24, and the analysis of specific storm events through multi-instrument data and models simulations, revealed the significant impact of the geomagnetic storm drivers in the observed effects [39,42,46–52]. Although it is known that ionospheric storm effects of significant intensity are observed even during solar minimum years, there is now some evidence that the ionospheric response to CIR/HSSs-driven storms may be different than the one to CME-driven events. In particular, it has been suggested that positive disturbances with strong afternoon components tend to be critical features of the ionospheric response to the impact of CIR/HSSs in the ionospheric middle latitudes, while these dominate during the declining phase and solar minimum conditions [47].

At first approach, the differences in the ionospheric storm-time response may be attributed to the intensity of the storm events: as CIR/HSSs drive geomagnetic storms of weak to moderate intensity, one would expect the generated neutral composition disturbance zone to be confined to higher latitudes. In any case, it may also be expected that the relative contribution of the ionospheric storm background mechanisms may differ between CME- and CIR/HSSs-driven disturbances, as the result of the differences in the total energy deposition into the auroral atmosphere [55–57], and the way in which this energy is distributed [15,58] during different storm scenarios. Of particular importance may be the role of the particle precipitation in the development of the ionospheric response during CIR/HSSs-driven disturbances [47]. The resulting heating may cause large-scale changes to the thermosphere composition, density and circulation (winds) in any case [21,59], but the rate of the energy deposition may differ between CME and CIR/HSSs cases [60]. It has been reported that the main phase of CME-driven events is characterized by intense but short-lived particle precipitation excursions, while the non-CME cases are characterized by prolonged periods of particle precipitation [47], which in turn may result in the gradual development of the disturbances and the limited extent of the neutral composition disturbance zone. In any case, the clarification of how the upper atmosphere is affected by solar coronal holes still requires the attention of the research community. Present availability in global-scale observations, new models and new analysis methods may facilitate systematic studies. The results, in combination with the output of studies on the CMEs that dominate solar maximum, would complete our understanding of storm time ionospheric response throughout the solar cycle [61], and would significantly advance our prediction capabilities in case it is proven that different storm scenarios need to be addressed differently by ionospheric prediction models [47,62,63].

A final point for further consideration when discussing ionospheric storm effects, is that it is not yet fully clarified whether foF2/NmF2 and TEC storm time responses always share the same features, and therefore, results obtained from the analysis of data from different data sources should be considered cautiously. TEC is defined as the integral of the entire ionospheric electron density profile. Such an integral has its maximum contribution from the F2 layer, with approximately 2/3 of the TEC coming from regions above the altitude (hmF2) of peak density (NmF2) [64]. Therefore, if substantial effects occur in TEC, simple vertical redistributions of F layer plasma cannot be the main cause [22]. In addition, in case the electron concentration at heights of the layer maximum is more sensitive to changes in thermospheric processes, and the effects of electrodynamics influence strongly higher altitudes which contribute substantially to the TEC estimates, one may expect quantitatively and maybe qualitatively different responses between foF2/NmF2 and TEC. Indeed, such discrepancies have been reported in the literature, such as, for instance, the results from the analysis of Chen et al. [65]. The authors conducted an epoch analysis of global ionosphere responses to recurrent geomagnetic activity during 79 corotating interaction region (CIR) events from 2004 to 2009 using GPS-derived TEC values, to find that in the high and middle latitudes, the TEC data showed a positive effect on the first storm day, while the negative response in the following days was only evident in the high latitudes. However, the daytime TEC response to CIR storms appeared to be different from that of ionospheric F2 peak densities at high and middle latitudes, as NmF2 had a long period of negative response for about 2–3 days, whereas the TEC response was mostly positive. Liu et al. [66], by conducting an analysis of the storm event of March 2015 at middle latitudes, reported SED signatures in TEC, but not in NmF2. Another example comes from the SWIF model scenarios: the comparative analysis of the variations in foF2 and TEC during eleven geomagnetic storm events that occurred in solar cycle 24 revealed similarities but also differences in the storm-time response of the two characteristics with respect to the local time and the latitude of the observation point. The most important difference concerns the intensity of positive storm effects, which appeared significantly greater in the TEC case. Moreover, positive storm effects at higher latitudes in case the observation point at storm onset time is located in the morning sector were present only

for TEC. The TEC positive phase was more intense in the lower latitudes, especially in the afternoon hours [67].

**Funding:** This research received no external funding.

**Institutional Review Board Statement:** Not applicable.

**Data Availability Statement:** Ionospheric observations were retrieved from the Global Ionosphere Radio Observatory (GIRO—http://giro.uml.edu/, accessed on 30 December 2021)) data repository, particularly FastChart database. Records of Dst index available by the World Data Center for Geomagnetism, Kyoto (http://wdc.kugi.kyoto-u.ac.jp/dstdir/, accessed on 30 December 2021). The smoothed monthly solar sunspot number is provided by the WDC-Sunspot Index and Long-Term Solar Observations (SILSO) in Royal Observatory of Belgium and the smoothed 10.7 cm radio flux provided by SWPC in NOAA.

**Conflicts of Interest:** The author declares no conflict of interest.

## References

1. Cander, L.R. *Ionospheric Storm Morphology. InIonospheric Space Weather*; Springer: Berlin/Heidelberg, Germany, 2019; pp. 95–133.
2. Schrijver, C.; Kauristie, K.; Aylward, A.D.; Denardini, C.M.; Gibson, S.E.; Glover, A.; Gopalswamy, N.; Grande, M.; Hapgood, M.; Heynderickx, D.; et al. Understanding space weather to shield society: A global road map for 2015–2025 commissioned by COSPAR and ILWS. *Adv. Space Res.* **2015**, *55*, 2745–2807. [CrossRef]
3. Kutiev, I.; Tsagouri, I.; Perrone, L.; Pancheva, D.; Mukhtarov, P.; Mikhailov, A.; Lastovicka, J.; Jakowski, N.; Buresova, D.; Blanch, E.; et al. Solar activity impact on the Earth's upper atmosphere. *J. Space Weather Space Clim.* **2013**, *3*, A06. [CrossRef]
4. Balan, N.; Yamamoto, M.; Liu, J.Y.; Otsuka, Y.; Liu, H.; Lühr, H. New aspects of thermospheric and ionospheric storms revealed by CHAMP. *J. Geophys. Res. Earth Surf.* **2011**, *116*, A07305. [CrossRef]
5. Reinisch, B.W.; Galkin, I.A. Global ionospheric radio observatory (GIRO). *EPS* **2011**, *63*, 377–381. [CrossRef]
6. Tsurutani, B.T.; Gonzalez, W.D.; Kamide, Y.; Arballo, J.K. (Eds.) *Magnetic Storms*; Geophysical Monograph Series; American Geophysical Union: Washington, DC, USA, 1997; Volume 98, p. 77. [CrossRef]
7. Suess, S.; Tsurutani, B.T. *From the Sun: Auroras, Magnetic Storms, Solar Flares, Cosmic Rays*; AGU Monograph: Washington, DC, USA, 1998.
8. Tsurutani, B.T.; McPherron, R.L.; Gonzalez, W.D.; Lu, G.; Sobral, J.H.A.; Gopalswamy, N. (Eds.) *Recurrent Magnetic Storms: Corotating Solar Wind Streams*; Geophysical Monograph Series; American Geophysical Union: Washington, DC, USA, 2006; Volume 167, ISBN 978-0-875-90432-0.
9. Hanslmeier, A. *The Sun and Space Weather, Springer Netherlands*, 2nd ed.; Astrophysics and Space Science Library: New York, NY, USA, 2007; Volume 347. [CrossRef]
10. Kamide, Y.; Chian, A. *Handbook of the Solar-Terrestrial Environment*; Springer: Berlin/Heidelberg, Germany, 2007.
11. Koskinen, H. *Physics of Space Storms: From the Solar Surface to the Earth*, 1st ed.; Springer: Berlin/Heidelberg, Germany, 2011. [CrossRef]
12. Buzulukova, N. *Extreme Events in Geospace, Origins, Predictability and Consequences*; Elsevier: Amsterdam, The Netherlands, 2018.
13. Tsurutani, B.T.; Lakhina, G.S.; Hajra, R. The physics of space weather/solar-terrestrial physics (STP): What we know now and what the current and future challenges are. *Nonlinear Process. Geophys.* **2020**, *27*, 75–119. [CrossRef]
14. Singh, A.; Bhargawa, A.; Siingh, D.; Singh, R. Physics of Space Weather Phenomena: A Review. *Geosciences* **2021**, *11*, 286. [CrossRef]
15. Hajra, R.; Echer, E.; Tsurutani, B.T.; Gonzalez, W.D. Solar wind-magnetosphere energy coupling efficiency and partitioning: HILDCAAs and preceding CIR storms during solar cycle 23. *J. Geophys. Res. Space Phys.* **2014**, *119*, 2675–2690. [CrossRef]
16. Dungey, J.W. Interplanetary Magnetic Field and the Auroral Zones. *Phys. Rev. Lett.* **1961**, *6*, 47–48. [CrossRef]
17. Perreault, P.; Akasofu, S.-I. A study of geomagnetic storms. *Geophys. J. Int.* **1978**, *54*, 547–573. [CrossRef]
18. Akasofu, S.-I. Interplanetary energy flux associated with magnetospheric substorms. *Planet. Space Sci.* **1979**, *27*, 425–431. [CrossRef]
19. Akasofu, S.-I. Energy coupling between the solar wind and the magnetosphere. *Space Sci. Rev.* **1981**, *28*, 121–190. [CrossRef]
20. Lastovicka, J. Monitoring and forecasting of ionospheric space weather—Effects of geomagnetic storms. *J. Atmos. Sol. -Terr. Phys.* **2002**, *64*, 697–705. [CrossRef]
21. Prölss, G.W. Density Perturbations in the Upper Atmosphere Caused by the Dissipation of Solar Wind Energy. *Surv. Geophys.* **2010**, *32*, 101–195. [CrossRef]
22. Mendillo, M. Storms in the ionosphere: Patterns and processes for total electron content. *Rev. Geophys.* **2006**, *44*, RG4001. [CrossRef]
23. Danilov, A. Ionospheric F-region response to geomagnetic disturbances. *Adv. Space Res.* **2013**, *52*, 343–366. [CrossRef]
24. Rishbeth, H. F-Region Storms and Thermospheric Dynamics. *J. Geomagn. Geoelectr.* **1991**, *43*, 513–524. [CrossRef]

25. Prölss, G.W. Ionospheric F region storms. In *Handbook of Atmospheric Electrodynamics*; Volland, H., Ed.; CRC Press: Boca Raton, FL, USA, 1995; pp. 195–248.
26. Fuller-Rowell, T.J.; Codrescu, M.V.; Moffett, R.J.; Quegan, S. Response of the thermosphere and ionosphere to geomagnetic storms. *J. Geophys. Res. Space Phys.* **1994**, *99*, 3893–3914. [CrossRef]
27. Buonsanto, M.J. Ionospheric storms—A review. *Space Sci. Rev.* **1999**, *88*, 563–601. [CrossRef]
28. Prölss, G.W. On explaining the local time variation of ionospheric storm effects. In *Annales Geophysicae*; Copernicus GmbH: Göttingen, Germany, 1993; Volume 11, pp. 1–9.
29. Tsurutani, B.T.; Verkhoglyadova, O.P.; Mannucci, A.J.; Saito, A.; Araki, T.; Yumoto, K.; Vasyliūnas, V.M. Prompt penetration electric fields (PPEFs) and their ionospheric effects during the great magnetic storm of 30–31 October 2003. *J. Geophys. Res. Space Phys.* **2008**, *113*, A05311. [CrossRef]
30. Foster, J.C.; Zou, S.; Heelis, R.A.; Erickson, P.J. Ionospheric Storm-Enhanced Density Plumes. In *Ionosphere Dynamics and Applications*; Huang, C., Lu, G., Zhang, Y., Paxton, L.J., Eds.; AGU Geophysical Monograph Series; American Geophysical Union: Washington, DC, USA, 2021; Volume 260, pp. 115–126.
31. Astafyeva, E.; Zakharenkova, I.; Förster, M. Ionospheric response to the 2015 St. Patrick's Day storm: A global multi-instrumental overview. *J. Geophys. Res. Space Phys.* **2015**, *120*, 9023–9037. [CrossRef]
32. Huba, J.D.; Sazykin, S.; Coster, A. SAMI3-RCM simulation of the 17 March 2015 geomagnetic storm. *J. Geophys. Res. Space Phys.* **2017**, *122*, 1246–1257. [CrossRef]
33. Nava, B.; Rodríguez-Zuluaga, J.; Alazo-Cuartas, K.; Kashcheyev, A.; Migoya-Orué, Y.; Radicella, S.; Amory-Mazaudier, C.; Fleury, R. Middle- and low-latitude ionosphere response to 2015 St. Patrick's Day geomagnetic storm. *J. Geophys. Res. Space Phys.* **2016**, *121*, 3421–3438. [CrossRef]
34. Astafyeva, E.; Bagiya, M.S.; Förster, M.; Nishitani, N. Unprecedented Hemispheric Asymmetries During a Surprise Ionospheric Storm: A Game of Drivers. *J. Geophys. Res. Space Phys.* **2020**, *125*, e2019JA027261. [CrossRef]
35. Astafyeva, E.; Zakharenkova, I.; Huba, J.D.; Doornbos, E.; Ijssel, J. Global Ionospheric and Thermospheric Effects of the June 2015 Geomagnetic Disturbances: Multi-Instrumental Observations and Modeling. *J. Geophys. Res. Space Phys.* **2017**, *122*, 11716–11742. [CrossRef]
36. Lei, J.; Huang, F.; Chen, X.; Zhong, J.; Ren, D.; Wang, W.; Yue, X.; Luan, X.; Jia, M.; Dou, X.; et al. Was Magnetic Storm the Only Driver of the Long-Duration Enhancements of Daytime Total Electron Content in the Asian-Australian Sector between 7 and 12 September 2017? *J. Geophys. Res. Space Phys.* **2018**, *123*, 3217–3232. [CrossRef]
37. Tsagouri, I.; Belehaki, A.; Moraitis, G.; Mavromichalaki, H. Positive and negative ionospheric disturbances at middle latitudes during geomagnetic storms. *Geophys. Res. Lett.* **2000**, *27*, 3579–3582. [CrossRef]
38. Burns, A.G.; Killeen, T.L.; Wang, W.; Roble, R.G. The solar-cycle-dependent response of the thermosphere to geomagnetic storms. *J. Atmos. Sol. -Terr. Phys.* **2004**, *66*, 1–14. [CrossRef]
39. Buresova, D.; Lastovicka, J.; Hejda, P.; Bochnicek, J. Ionospheric disturbances under low solar activity conditions. *Adv. Space Res.* **2014**, *54*, 185–196. [CrossRef]
40. Fuller-Rowell, T.; Araujo-Pradere, E.; Codrescu, M. An empirical ionospheric storm-time correction model. *Adv. Space Res.* **2000**, *25*, 139–146. [CrossRef]
41. Araujo-Pradere, E.A.; Fuller-Rowell, T.J.; Codrescu, M.V. STORM: An empirical storm-time ionospheric correction model: 1. Model description. *Radio Sci.* **2002**, *37*, 1–12.
42. Wang, W.; Wiltberger, M.; Burns, A.G.; Solomon, S.C.; Killeen, T.L.; Maruyama, N.; Lyon, J.G. Initial results from the coupled magnetosphere-ionosphere-thermosphere model: Thermosphere-ionosphere responses. *J. Atmos. Sol. -Terr. Phys.* **2004**, *66*, 1425–1441. [CrossRef]
43. Tsagouri, I.; Belehaki, A. A new empirical model of middle latitude ionospheric response for space weather applications. *Adv. Space Res.* **2006**, *37*, 420–425. [CrossRef]
44. Tsagouri, I.; Belehaki, A. An upgrade of the solar-wind-driven empirical model for the middle latitude ionospheric storm-time response. *J. Atmos. Sol. -Terr. Phys.* **2008**, *70*, 2061–2076. [CrossRef]
45. Tsagouri, I.; Koutroumbas, K.; Belehaki, A. Ionospheric foF2 forecast over Europe based on an autoregressive modeling technique driven by solar wind parameters. *Radio Sci.* **2009**, *44*, 1–21. [CrossRef]
46. Tsagouri, I.; Belehaki, A. Ionospheric forecasts for the European region for space weather applications. *J. Space Weather Space Clim.* **2015**, *5*, A9. [CrossRef]
47. Tsagouri, I.; Galkin, I.; Asikainen, T. Long-term changes in space weather effects on the Earth's ionosphere. *Adv. Space Res.* **2017**, *59*, 351–365. [CrossRef]
48. Burns, A.G.; Solomon, S.C.; Qian, L.; Wang, W.; Emery, B.A.; Wiltberger, M.; Weimer, D.R. The effects of corotating interaction region/high speed stream storms on the thermosphere and ionosphere during the last solar minimum. *J. Atmos. Sol. -Terr. Phys.* **2012**, *83*, 79–87. [CrossRef]
49. Dmitriev, A.V.; Huang, C.M.; Brahmanandam, P.S.; Chang, L.C.; Chen, K.T.; Tsai, L.C. Longitudinal variations of positive dayside ionospheric storms related to recurrent geomagnetic storms. *J. Geophys. Res. Space Phys.* **2013**, *118*, 6806–6822. [CrossRef]
50. Verkhoglyadova, O.; Tsurutani, B.T.; Mannucci, A.J.; Mlynczak, M.G.; Hunt, L.A.; Runge, T. Variability of ionospheric TEC during solar and geomagnetic minima (2008 and 2009): External high speed stream drivers. *Ann. Geophys.* **2013**, *31*, 263–276. [CrossRef]

51. Verkhoglyadova, O.P.; Tsurutani, B.T.; Mannucci, A.J.; Mlynczak, M.G.; Hunt, L.A.; Komjathy, A.; Runge, T. Ionospheric VTEC and thermospheric infrared emission dynamics during corotating interaction region and high-speed stream intervals at solar minimum: 25 March to 26 April 2008. *J. Geophys. Res. Space Phys.* **2011**, *116*, A09325. [CrossRef]
52. Matamba, T.M.; Habarulema, J.B. Ionospheric Responses to CME- and CIR-Driven Geomagnetic Storms Along 30 °E–40 °E Over the African Sector From 2001 to 2015. *Space Weather* **2018**, *16*, 538–556. [CrossRef]
53. Prölss, G.W. Ionospheric Storms at Mid-Latitude: A Short Review. *Midlatitude Ionos. Dyn. Disturb.* **2018**, *181*, 9–24. [CrossRef]
54. Fuller-Rowell, T.; Yizengaw, E.; Doherty, P.H.; Basu, S. *Ionospheric Space Weather: Longitude Dependence and Lower Atmosphere Forcing*; John Wiley and Sons: Hoboken, NJ, USA, 2016; Volume 220.
55. Kozyra, J.U.; Crowley, G.; Emery, B.A.; Fang, X.; Maris, G.; Mlynczak, M.G.; Niciejewski, R.J.; Palo, S.E.; Paxton, L.J.; Randall, C.E. Response of the Upper/Middle Atmosphere to Coronal Holes and Powerful High-Speed Solar Wind Streams in 2003. In *Recurrent Magnetic Storms: Corotating Solar Wind Streams*; AGU Geophysical Monograph Series; Tsurutani, B.T., McPherron, R.L., Gonzalez, W.D., Lu, G., Sobral, J.H.A., Gopalswamy, N., Eds.; American Geophysical Union: Washington, DC, USA, 2006; Volume 167, p. 319. [CrossRef]
56. Turner, N.E.; Mitchell, E.J.; Knipp, D.J.; Emery, B.A. Energetics of magnetic storms driven by corotating interaction regions: A study of geoeffectiveness. In *Recurrent Magnetic Storms, Corotating Solar Wind Streams*; Geophysical Monograph, Series; Tsurutani, B.T., McPherron, R., Gonzalez, W., Lu, G., Sobral, J.H.A., Gopalswamy, N., Eds.; AGU: Washington, DC, USA, 2006; Volume 167, pp. 113–124.
57. Verkhoglyadova, O.P.; Mannucci, A.J.; Tsurutani, B.T.; Mlynczak, M.G.; Hunt, L.A.; Redmon, R.J.; Green, J.C. Localized thermosphere ionization events during the high-speed stream interval of 29 April to 5 May 2011. *J. Geophys. Res. Space Phys.* **2014**, *120*, 675–696. [CrossRef]
58. Emery, B.A.; Richardson, I.; Evans, D.S.; Rich, F.J. Solar wind structure sources and periodicities of auroral electron power over three solar cycles. *J. Atmos. Sol. -Terr. Phys.* **2009**, *71*, 1157–1175. [CrossRef]
59. Mannucci, A.J.; Verkhoglyadova, O.P.; Tsurutani, B.T.; Meng, X.; Pi, X.; Wang, C.; Rosen, G.; Lynch, E.; Sharma, S.; Ridley, A.; et al. Medium-Range Thermosphere-Ionosphere Storm Forecasts. *Space Weather* **2015**, *13*, 125–129. [CrossRef]
60. Longden, N.; Denton, M.H.; Honary, F. Particle precipitation during ICME-driven and CIR-driven geomagnetic storms. *J. Geophys. Res. Earth Surf.* **2008**, 113. [CrossRef]
61. Mannucci, A.J.; Tsurutani, B.T.; Solomon, S.C.; Verkhoglyadova, O.P.; Thayer, J.P. How Do Coronal Hole Storms Affect the Upper Atmosphere? *Eos* **2012**, *93*, 77–79. [CrossRef]
62. Aa, E.; Zhang, S.R.; Erickson, P.J.; Coster, A.J.; Goncharenko, L.P.; Varney, R.H.; Eastes, R. Salient Midlatitude Ionosphere-Thermosphere Disturbances Associated with SAPS During a Minor but Geo-Effective Storm at Deep Solar Minimum. *J. Geophys. Res. Space Phys.* **2021**, *126*, e2021JA029509. [CrossRef]
63. Qiu, N.; Chen, Y.H.; Wang, W.B.; Gong, J.C.; Liu, S.Q. Statistical analysis of the ionosphere response to the CIR and CME in Mid-latitude regions. *Chin. J. Geophys.* **2015**, *58*, 2250–2262.
64. Belehaki, A.; Tsagouri, I. Investigation of the relative bottomside/topside contribution to the total electron content estimates. *Ann. Geophys.* **2009**, *45*, 73–86. [CrossRef]
65. Chen, Y.; Liu, L.; Le, H.; Wan, W. Geomagnetic activity effect on the global ionosphere during the 2007–2009 deep solar minimum. *J. Geophys. Res. Space Phys.* **2014**, *119*, 3747–3754. [CrossRef]
66. Liu, J.; Wang, W.; Burns, A.; Yue, X.; Zhang, S.; Zhang, Y.; Huang, C. Profiles of ionospheric storm-enhanced density during the 17 March 2015 great storm. *J. Geophys. Res. Space Phys.* **2015**, *121*, 727–744. [CrossRef]
67. Tsagouri, I.; Koutroumbas, K.; Elias, P. A new short-term forecasting model for the total electron content storm time disturbances. *J. Space Weather Space Clim.* **2018**, *8*, A33. [CrossRef]